Proceedings of the 2007 IEEE/RSJ International
Conference on Intelligent Robots and Systems
San Diego, CA, USA, Oct 29 - Nov 2, 2007

WeC2.1

Modeling and Rendering Contact Torques and Twisting Effects of Deformable Objects in Haptic Interaction*

Qi Luo and Jing Xiao

IMI Lab, Department of Computer Science
University of North Carolina - Charlotte
Charlotte, NC 28223, USA
{qluo, xiao}@uncc.edu

Abstract— Contact and deformation modeling for interactive environments has seen many applications, from surgical simulation and training, to virtual prototyping, to teleoperation, etc., where both visual feedback and haptic feedback are needed in real-time (kHz). In this paper, we consider contacts between a rigid body and an elastic object and address a little studied problem: the modeling and rendering of compliant twisting or rotation of the rigid body on the surface of the elastic object and the associated effects in the deformation of the elastic object. We present a unique strategy to model the contact torques applied to the rigid body and the resulted shape deformation of the elastic object. This strategy extends the general paradigm of contact and deformable modeling introduced by the authors earlier [1] so that not only contact forces but also contact torques, not only compliant translations but also compliant rotations of the rigid body, as well as the resulted deformations of the elastic object can all be simulated in a combined update rate of over 1kHz. The strategy is implemented, and the experimental results confirm its effectiveness and efficiency.

Index Terms— twisting effect, deformable object, haptic rendering, contact torque, multiple contacts

I. INTRODUCTION

Modeling deformable objects in contact has been studied both for graphic rendering and for haptic rendering. Gibson and Mirtich [2] provided a very detailed and complete survey on deformable modeling used in graphic rendering. More recent surveys on graphic and haptic rendering involving deformable objects can be found in [3][4]. While graphic rendering only needs to make the modeled object deformation *looks* realistic, haptic rendering requires that the deformed object *feels* realistic as well. While the update rate in graphic rendering needs to be around 20–30 Hz to look realistic, the update rate in haptic rendering needs to reach 1kHz to feel realistic. Therefore, haptic rendering has a much more stringent requirement than graphic rendering to achieve high rendering quality, which is essential for many applications that simulate manipulations or interactions in real physical world.

In order to achieve high haptic rendering rate, existing approaches often apply certain simplifications to the physically-based deformable models used in graphic rendering, such as mass-spring-damper models and continuum models, and

focus on simple contact cases. Most of the approaches are focused on single point contact [5][6][7][8][9], single-area contact [10][11][12], and localized deformation [13]. Recently, the authors introduced a general approach [1][14] to contact force and deformable modeling for complex contacts between a rigid body and an elastic object that can involve multiple contact regions and compliant translations of the rigid body with friction. The approach detects multi-region contacts, simulates contact forces, simulates and renders both local and global deformations of the elastic object in a combined update rate of over 1kHz.

When there are rotations between two contacting objects, there are contact torques. If a held virtual object compliantly twists or rotates on the surface of another virtual object, the human operator should feel contact torques to the held object from the other object via haptic rendering. There exists research on rendering contact torques between rigid objects for display with a six or higher degrees-of-freedom haptic device[15] [16] [17] [18]. Once contact forces are modeled, contact torques can be computed from the contact forces and the contact points rather easily for rigid objects. Some researchers modeled contact torques from contacts for haptic rendering involving deformable objects [19][20]. However, there is little research on modeling both contact torques and the corresponding twisting effects on shape deformation for real-time haptic rendering when a deformable object is involved in contacts.

This paper addresses the problem of both contact torque modeling and shape deformation modeling real-time for complex contacts between a rigid body and an elastic object involving twisting or compliant rotations. It presents an effective and efficient strategy suitable for haptic interaction and substantially extends the framework introduced in [1][14] that do not consider compliant rotations, contact torques, and the corresponding twisting effects on shape deformation.

The rest of the paper is organized as follows. In section II, we review the general approach for contact detection, contact force modeling, and deformation modeling introduced in [1][14], where no contact torques and effects are considered. In sections III, IV, and V, we present our strategy for modeling contact torques and the shape deformation due to compliant twisting or rotation for both single-region

and multi-region contacts. We present some implementation results in section VI and conclude the paper in section VII.

II. REVIEW OF RELATED WORK

This section briefly reviews the approach for contact and deformation modeling between a rigid body and an elastic objects introduced earlier [1][14] since the strategy of this paper extends that approach by modeling contact torques, compliant rotation, and the corresponding effects on shape deformation.

A. Basic Assumptions

Contacts are considered between a rigid object and an elastic object in a virtual environment. A mesh model representation is used for the geometry of the rigid object. Mesh models are also used to represent the elastic object in its original undeformed shape and in deformed shapes. The elastic object considered is convex when undeformed, and there is a parametric model of the originally undeformed surface.

The rigid object is virtually held by a human user via a haptic device. Here the force exerted to the held object from the human user is assumed to apply to the mass center of the held object. This assumption is useful for estimating the distribution of contact pressure.

A single *contact region* is defined as a set of contact points S such that the distance between a contact point in S and its nearest neighboring contact point in S is less than a threshold r_{th}. A contact point outside S is considered belonging to another contact region, and there can be multiple contact regions in general.

The study only focuses on cases where each single contact region is relatively small so that within the contact region, the first partial derivatives of the originally undeformed surface of the elastic object hardly change. A contact region may consist of just a single contact point.

There can be multiple contact regions between the rigid object and the elastic object at the same time, but multiple contact regions are assumed to be formed one by one.

Only quasi-static contacts and compliant motion are considered. This means that motions considered are slow enough such that deformation occurring at only stable equilibrium configurations, where the elastic energy is minimized. This provides an effective discretization of the otherwise continuous force and shape changes on the elastic object in contact.

B. Real-Time Contact Detection

While collision detection is concerned with whether or not there is a collision, contact detection is also concerned with *where* and *how hard* a collision happens. Contact detection is not a fully solved problem when deformable objects and multiple contacts are involved. Our strategy for contact detection between a rigid body and a deformable object is as follows: First, test for collision as if between two rigid bodies. Once a contact happens, dynamically update the surface model of the elastic object and use an existing collision detection package SOLID [21] to detect the penetration distance between two objects. However, since SOLID can only track one contact at each time step, our method dynamically divides the elastic object into multiple parts and applies SOLID to detect contacts between the rigid object and each part of the elastic object.

C. Contact Force and Shape Deformation Modeling

The approach reported in [1] can handle complex contact states between a rigid body and an elastic object with multiple contact regions and compliant translations with friction.

A nonlinear model is used to simulate contact forces exerted to the held rigid object from the elastic object under point contact, and the model is extended to general non-point contacts without or with compliant translations of the held object under friction.

Both global deformation of the entire elastic object and local deformation within neighborhoods of contact regions are modeled. In order to handle the global shape change due to deformation, a novel 'beam-skeleton model' with respect to a contact region is introduced to compute the distribution of stresses and strains of a deformed elastic object at certain 'anchor points' defined on the original, undeformed surface of the object. Based on this model, fast computation of global shape change is realized through an interpolation method that achieves minimization of the elastic energy. Next the model for shape deformation further takes into account nonlinear effects within local neighborhoods of contact regions and the effects of different areas of contact regions (under the same force) on shape change.

Both contact force and shape deformation effects of multiple contact regions are modeled by building beam-skeletons and computing shape deformation based on the temporal order of contact regions (since contact regions are assumed to be formed one by one).

III. CONTACT TORQUE MODELING

When a held rigid object rotates while in contact with an elastic object, and the rotation axis does not go through a contact region, the contact torque T applied from this contact region on the elastic object to the held rigid object can be simply calculated as

$$T = \mathbf{r} \times \mathbf{F} \qquad (1)$$

where $\mathbf{F}$ is the contact force to the rigid object from the contact region and $\mathbf{r}$ is the distance vector from the (equivalent) contact point [1] to the rotation axis, which goes through the mass center of the rigid object according to the assumption (in section II.A).

When the rotation axis goes through a contact region, as shown in Fig. 1, the friction from the elastic object provides

---

[1]An *equivalent point contact* to a single region contact is defined such that the contact force response to that point contact is the same as the total contact force response of the single region contact. Using such an equivalence of a point contact to the original single region contact simplifies the graphical shape rendering of the deformed elastic object. Further details can be found in [1] and [14].
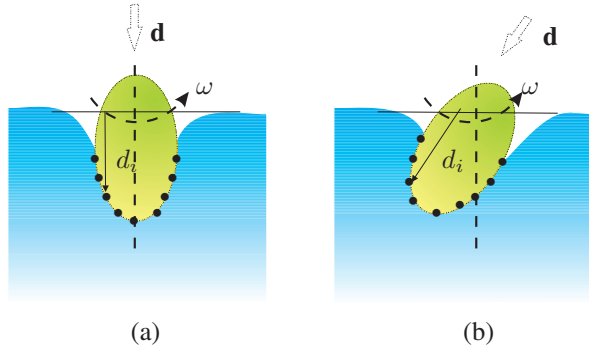
Fig. 1. Examples of single-region contact: (a) rotation axis (dashed straight line) along **d**, the direction of deformation, (b) rotation axis is different from **d**

Fig. 2. Side view of a twisting elastic object under a rotation of a rigid object

a torque T to the rigid object. This torque is in fact the torque of the elastic object's twisting shear stress.

To compute this torque T, we discretize the contact region of the rigid object into n small regions $s_1, ..., s_n$. Each $s_i, i = 1, ..., n$ is centered at contact point p_i on the rigid object and has a constant area Δs. We first compute the torsional force $\mathbf{F}_{t_i}$ exerted on p_i following the approach in [1][14], and then compute the torque T_i from $\mathbf{F}_{t_i}$, and finally sum up all T_i to obtain T.

Let r_i be the distance between p_i and the rotation axis of the held rigid object. Let ℓ_i be the projection of distance from p_i to the fixed point q_f of the elastic object along the rotation axis, and let q_i be the contact point on the elastic object corresponding to p_i.

The friction from p_i to q_i may make q_i stick to p_i when p_i rotates. If p_i rotates the angle φ_{p_i}, then q_i sticks to p_i (i.e., rotates with p_i) if the twisting shear stress τ_{t_i} on q_i satisfies the following:

$$\tau_{t_i} = r_i G \Phi_{p_i} \qquad (2)$$

where $\Phi_{p_i} = \varphi_{p_i}/\ell_i$. G is the shear modulus of elasticity, which is related to the Young's modulus E and the Poisson's ratio ν [22]:

$$G = \frac{E}{2(1+\nu)} \qquad (3)$$

Now we look at how q_i exerts frictional torque T_i to p_i and how this torque is computed. Let $\Delta f_{max} = f_{max}/n$ be the maximum static friction on each small contact region of the rigid object (recall that we discretize the contact region of the rigid object into n small regions). Let $\Delta f_D = f_D/n$ denotes the kinetic friction on each small contact region of the rigid object, where $f_D = \mu_D \mathbf{F_n}$, μ_D is the dynamic friction coefficient, and $\mathbf{F_n}$ is the normal component of the contact force as obtained in the case of contact without rotation [1][14].

First consider that the rigid object does not translate. q_i sticks to p_i if $\Delta f_{max} \geq \tau_{t_i}\Delta s$, and the corresponding $\mathbf{F_{t_i}}$ applied to p_i satisfies
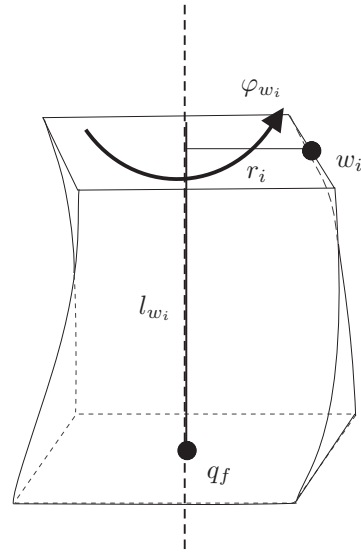
$$\mathbf{F}_{t_i} = \tau_{t_i}\Delta s \qquad (4)$$

Otherwise, there is a relative motion between q_i and p_i, and we have

$$\mathbf{F}_{t_i} = \Delta f_D \qquad (5)$$

Note that from equation (2), the part of the contact region on the elastic object that moves together with the rigid object has the maximum radius r_{m_s} as

$$r_{m_s} = \frac{\Delta f_{max}}{G \Phi_{p_i} \Delta s} \qquad (6)$$

when the rigid object does not translate.

Now consider that the rigid object translates. In this case, there is a relative motion between any pair of p_i and q_i. Let $r_{m_d} = \frac{\Delta f_D}{G \Phi_{p_i} \Delta s}$, then $\mathbf{F}_{t_i}$ applied to p_i satisfies

$$\mathbf{F}_{t_i} = \begin{cases} \tau_{t_i}\Delta s & r_i \leq r_{m_d} \\ \Delta f_D & r_i > r_{m_d} \end{cases} \qquad (7)$$

Therefore, the contact torque T_i applied from q_i to the held rigid object is

$$T_i = \begin{cases} \mathbf{r}_i \times \tau_{t_i}\Delta s & r_i \leq r_m \\ \mathbf{r}_i \times \Delta f_D & r_i > r_m \end{cases} \qquad (8)$$

where $r_m = r_{m_s}$ if there is no translation or $r_m = r_{m_d}$ otherwise.

The total contact torque applied to the held rigid object from a contact region where the rotation axis (of the held object) goes through is the sum:

$$T = \sum_{i=1}^{n} T_i \qquad (9)$$

IV. TWISTING EFFECTS ON SHAPE DEFORMATION

When the rigid object rotates while contacting the elastic object, the shape deformation of the elastic object due to twisting needs to be considered. As shown in Fig. 2, assume that the elastic object has one fixed point q_f. If the rotation axis does not go through the contact region, the twisting effect on the shape deformation of the elastic object can be rendered by computing how much a point on the elastic object rotates as the rigid object rotates. Let w_i be a point on the elastic object, which can be either a contact point or a non-contact point. Let the rotation angle of w_i be φ_{w_i}, the distance from w_i to the rotation axis be r_{w_i}, and ℓ_{w_i} be the projection of the distance from w_i to q_f along the rotation axis. φ_{w_i} can be computed in the following way:

$$\varphi_{w_i} = \frac{||T|| \ell_{w_i}}{r_{w_i} G} \quad (10)$$

When the rotation axis goes through a contact region that is formed between two objects, a contact point q_i on the elastic object may or may not move together with the rotating rigid object, as discussed in section III. The shape deformation due to torsional effect can be rendered by computing whether and how much q_i rotates as the corresponding contact point p_i on the rigid object rotates. Let the angle of rotation of q_i be φ_{q_i} when p_i rotates φ_{p_i}, the distance from q_i to the rotation axis be r_{q_i}, and ℓ_{q_i} be the distance from q_i along the rotation axis to q_f. φ_{q_i} can be computed in the following way.

If the rigid object only rotates, then

$$\varphi_{q_i} = \begin{cases} \varphi_{p_i} & r_{q_i} \leq r_{m_s} \\ \frac{\Delta f_D \ell_{q_i}}{r_{q_i} G \Delta s} & r_{q_i} > r_{m_s} \end{cases} \quad (11)$$

Fig. 3 illustrates the rotation angle for two points q_i and q_j, where $r_{q_i} \leq r_{m_s}$ and $r_{q_j} > r_{m_s}$.

If the rigid object translates on the surface of the elastic object, then

$$\varphi_{q_i} = \begin{cases} \frac{\tau_t \ell_{q_i}}{r_{q_i} G} & r_{q_i} \leq r_{m_d} \\ \frac{\Delta f_D \ell_{q_i}}{r_{q_i} G \Delta s} & r_{q_i} > r_{m_d} \end{cases} \quad (12)$$

For any non-contact point u_i on the elastic object, its twisting shape deformation is due to the stress force and can be computed as the following:

$$\varphi_{u_i} = \begin{cases} \frac{r_{m_s} \varphi_{m_s}}{r_{u_i}} & pure \quad rotation \\ \frac{r_{m_d} \varphi_{m_d}}{r_{u_i}} & with \quad translation \end{cases} \quad (13)$$

where r_{u_i} is the distance between u_i and the rotation axis. φ_{m_s} and φ_{m_d} are rotation angles of any point with radius r_{m_s} and r_{m_d}, respectively.

V. DEALING WITH MULTIPLE CONTACT REGIONS

When multiple contact regions are formed between a held rigid object and an elastic object, we can obtain the contact force and the corresponding beam-skeleton for each contact region [1].
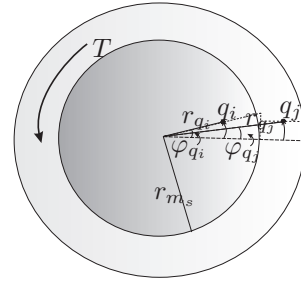

Fig. 3. Top view of a contact region on the elastic object under a rotation of the rigid object

If the held object rotates with the rotation axis not going through any contact region, the total contact torque T_c is the sum of the torques from all contact regions, each of which can be calculated as in Eq. 1.

If the rotation axis goes through a contact region C_m, because of the twisting effects from other contact regions, all contact points of C_m, $q_i, i = 1, ..., n$, on the elastic object now have relative motions with respect to the rigid object. Therefore, friction at every q_i becomes dynamic, and the contact torque applied to the rigid object from C_m should be recalculated as

$$T_{c_m} = \sum_{i=1}^{n} (\mathbf{r}_i \times \Delta f_D) \quad (14)$$

The total contact torque T_c is obtained by adding T_{c_m} to the sum of contact torques from every other contact region (where the rotation axis does not go through).

To render the twisting shape deformation under multiple contact regions, the rotation angle of any point on the elastic object is computed as the sum of twisting angles of this point due to the twisting effect of each individual contact region.

VI. IMPLEMENTATION AND TEST RESULTS

We have implemented the above method and applied it to real-time haptic rendering involving a virtual rigid body and an elastic object via a PHANToM Premium 1.5/6DOF device, which is connected to a personal computer with dual Intel Xeon 2.4GHz Processors and 1GB system RAM. The human operator can virtually hold the rigid object A by attaching it to the haptic device and make arbitrary contact to the elastic object B (with its bottom center fixed, where a world coordinate system is set) by guarded motions and perform compliant motions on the elastic object. The haptic simulation is quite stable under quasi-static compliant motions.

Note that in our approach, the time for the haptic force and torque modeling and rendering is negligible compared to the time needed for real-time contact detection. Real-time haptic rendering can be achieved with a reasonable number of contact regions (≤ 10). Adding the strategy of contact torque modeling and twisting deformation modeling introduced in this paper to the general contact force and deformation modeling approach introduced in [1][14], we

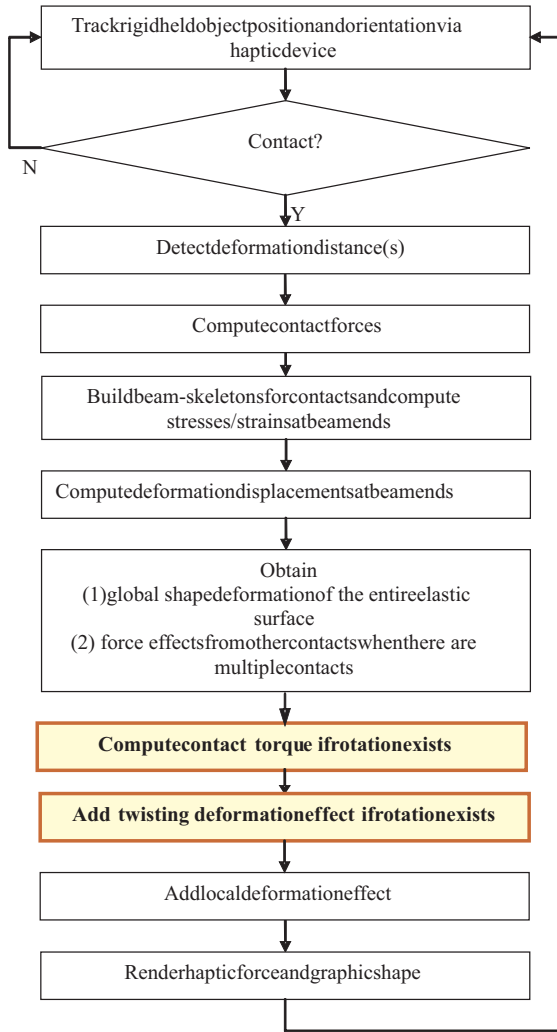can extend the flowchart of the general approach (for one time step) as shown in Fig. 4.

Fig. 4. Overview of approach (one time step per loop) - the highlighted boxes indicate the work described in this paper

Parameter	Value	Parameter	Value
$m(kg)$	1.0	$E(N/m^2)$	$3 \cdot 10^6$ [a]
μ_D	0.75	ν	0.5 [a]
$\rho(kg/m^2)$	1100 [a]		

[a]Parameters of Rubber
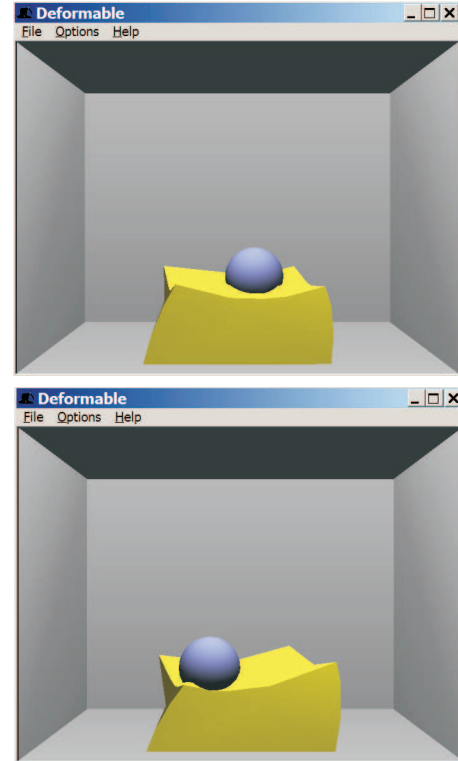
Fig. 5. Example of twisting effects under torsional torques

Table I lists the parameters used in our experiments.

Fig. 5 shows an experiment, where the rigid held ball rotates, and the twisting effect on the shape deformation of the elastic cube is rendered. A video clip of this experiment is also attached to this paper. Note that the ball may *appear* to penetrate into the elastic cube but this appearance is only due to the large deformation of the elastic cube; there is actually no penetration.

Fig. 6 shows another experiment of the twisting effects on the shape of the elastic ellipsoid under different torsional torques as the held rigid mallet rotates clockwise and counter-clockwise respectively.

Fig 7 shows an experiment of twisting deformation under multiple contact regions, where the held rigid compass contacts an elastic ellipsoid in two contact regions.

In all the experiments, our algorithm achieves a combined update rate of over 1kHz for all the modeling and rendering (depicted in Fig. 4).

VII. CONCLUSIONS

We have introduced a unique strategy to model and render in real-time the contact torque applied to a rigid body as it rotates on the surface of an elastic object and the associated effects in the deformation of the elastic object. This approach has been implemented to confirm its effectiveness and efficiency.

REFERENCES

[1] Q. Luo and J. Xiao, "Contact and deformation modeling for interactive environments," *IEEE Transactions on Robotics, in press*, 2007.
[2] S. Gibson and B. Mirtich, "A survey of deformable modeling in computer graphics," Tech. Report No. TR-97-19, Mitsubishi Electric Research Lab., Cambridge,MA, November 1997.
[3] J. Lang, *Deformable Model Acquisition and Validation*. Ph.D. thesis, The University of British Columbia, October 2001.
[4] A. Al-khalifah and D. Roberts, "Survey of modelling approaches for medical simulators," in *Proc. 5th Intl Conf. Disability, Virtual Reality and Assoc. Tech.*, (Oxford, UK), pp. 321–329, 2004.
[5] D. Aulignac, R. Balaniuk, and C. Laugier, "A haptic interface for a virtual exam of the human thigh.," in *Proc. of IEEE International Conference on Robotics and Automation*, pp. 2452–2457, 2000.
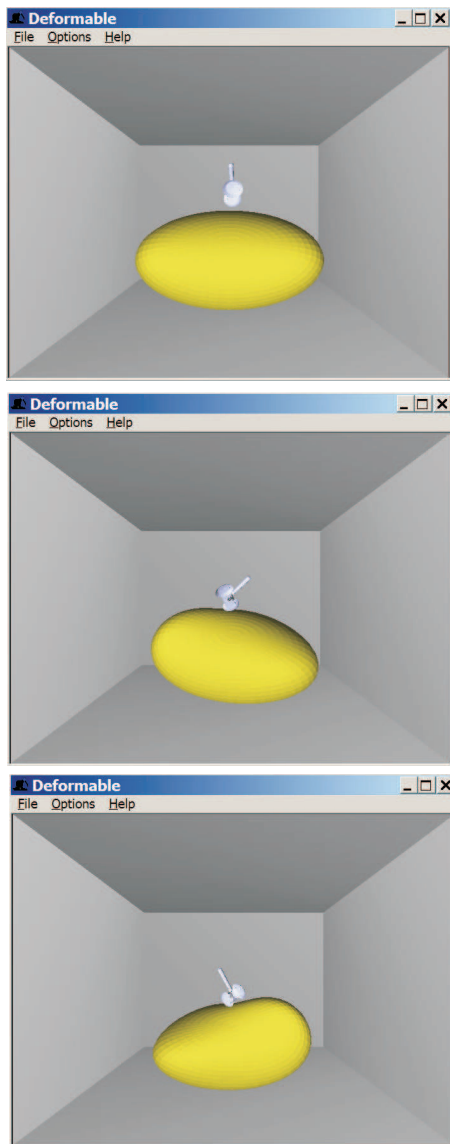
Fig. 7. Twisting deformation under two contact regions

Fig. 6. Another example of twisting effects: (top) undeformed shape, (middle) shape deformed under clockwise torsional torque, (bottom) shape deformed under counter-clockwise torsional torque
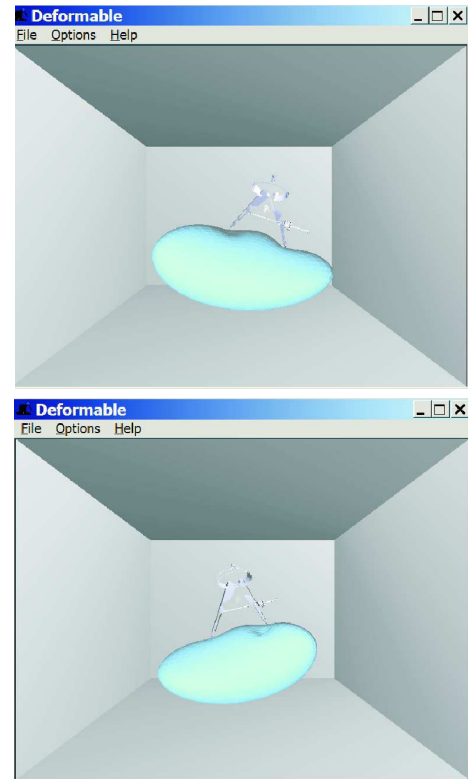
[6] M. Bro-Nielsen, "Finite element modeling in surgery simulation.," vol. 86, no. 3, pp. 490–503, 1998.

[7] S. Cotin, H. Delingette, and N. Ayache, "Real-time elastic deformations of soft tissues for surgery simulation," *IEEE Transactions on Visualization and Computer Graphics*, vol. 5, pp. 62–73, January-March 1999.

[8] D. Nelson, D. Johnson, and E. Cohen, "Haptic rendering of surface-to-surface sculpted model interaction.," in *Proc. of the Symposium on Haptic Interfaces for Virtual Environments and Teleoperator Systems*, pp. 101–108, 1999.

[9] Y. Zhuang and J. Canny, "Haptic interaction with global deformations," in *Proc. of IEEE Int. Conf. on Robotics and Automation*, pp. 2428–2433, April 2000.

[10] G. Debunne, M. Desbrun, M. Cani, and A. Barr, "Dynamic real-time deformations using space and time adaptive sampling," in *Computer Graphics and Interactive Techniques, SIGGRAPH 2001*, pp. 31–36, ACM Press, 2001.

[11] D. James and D. Pai, "A unified treatment of elastostatic contact simulation for real-time haptics," *haptics-e*, vol. 2, no. 1, pp. 1–13, 2001.

[12] X. Wu, M. Downes, T. Goktekin, and F. Tendick, "Adaptive nonlinear finite elements for deformable body simulation using dynamic progressive meshes," *EUROGRAPHICS 2001*, vol. 20, no. 3, pp. 349–358, 2001.

[13] M. Mahvash and V. Hayward, "High-fidelity haptic synthesis of contact with deformable bodies," *IEEE Computer Graphics and Applications*, vol. 24, pp. 48–55, Feb. 2004.

[14] Q. Luo and J. Xiao, "Modeling complex contacts involving deformable objects for haptic and graphic rendering," in *Proceedings of Robotics: Science and Systems 2005*, (MIT Press), June 2005.

[15] W. McNeely, K. Puterbaugh, and J. Troy, "Six degree-of-freedom haptic rendering using voxel sampling," in *Proceedings of the 26th annual conference on Computer graphics and interactive techniques*, pp. 401–408, 1999.

[16] A. Gregory, A. Mascarenhas, S. Ehmann, M. Lin, and D. Manocha, "Six degrees-of-freedom haptic display of polygonal models," in *11th IEEE Visualization 2000 (VIS'00)*, pp. 139–146, 2000.

[17] S. Wang and M. Srinivasan, "The role of torque in haptic perception of object location in virtual environments," in *Proceedings of the11th Symposium on Haptic Interfaces for Virtual Environment and Teleoperator Systems (HAPTICS03)*, pp. 302–309, 2003.

[18] Q. Luo and J. Xiao, "Physically accurate haptic rendering with dynamic effects," *IEEE Computer Graphics and Applications, Special Issue -Touch-Enabled Interfaces*, vol. 24, no. 6, Nov/Dec. 2004.

[19] C. Basdogan, S. De, J. Kim, M. Muniyandi, H. Kim, and M. Srinivasan, "Haptic in minimally invasive surgical simulation and training," *Computer Graphics and Applications*, pp. 56–64, March/April 2004.

[20] C. Duriez, F. Dubois, K. Abderrahmane, and C. Andriot, "Realistic haptic rendering of interacting deformable objects in virtual environments," *IEEE Transactions on Visualization and Computer Graphics*, vol. 12, no. 1, pp. 36–47, 2006.

[21] G. Bergen, "Efficient collision detection of complex deformable models using aabb trees," *J. of Graphics Tools*, vol. 2, no. 4, pp. 1–13, 1997.

[22] J. Smith and O. Sidebottom, *Elementary Mechanics of Deformable Bodies*. The Macmillan Company, 1969.